Received: 16 January 2023 | Revised: 15 February 2023 | Accepted: 17 February 2023

DOI: 10.1002/ardp.202300029

FULL PAPER

ARCH PHARM DPhG
Archiv der Pharmazie

5,6-Dihydrotetrazolo[1,5-*c*]quinazolines: Toxicity prediction, synthesis, antimicrobial activity, molecular docking, and perspectives

Lyudmyla Antypenko[1] | **Oleksii Antypenko**[2] | **Iryna Karnaukh**[3] | **Oksana Rebets**[3] | **Sergiy Kovalenko**[4] | **Mieko Arisawa**[1]

[1]Department of Bioscience and Biotechnology, Graduate School of Bioresource and Bioenvironmental Sciences, Kyushu University, Fukuoka, Japan

[2]Department of Pharmaceutical, Organic and Bioorganic Chemistry, Zaporizhzhia State Medical University, Zaporizhzhia, Ukraine

[3]Bacteriological Laboratory, Zaporizhzhia Regional Hospital, Zaporizhzhia, Ukraine

[4]Research Institute of Chemistry and Geology, Oles Honchar Dnipro National University, Dnipro, Ukraine

Correspondence
Lyudmyla Antypenko, Department of Bioscience and Biotechnology, Graduate School of Bioresource and Bioenvironmental Sciences, Kyushu University, Fukuoka 819-0395, Japan.
Email: antypenkol@gmail.com

Abstract

Antimicrobial resistance is a never-ending challenge, which should be considered seriously, especially when using unprescribed "over-the-counter" drugs. The synthesis and investigation of novel biologically active substances is among the directions to overcome this problem. Hence, 18 novel 5,6-dihydrotetrazolo[1,5-*c*]quinazolines were synthesized, their identity, purity, and structure were elucidated by elemental analysis, IR, LC-MS, ^{1}H, and ^{13}C NMR spectra. According to the computational estimation, 15 substances were found to be of toxicity Class V, two of Class IV, and only one of Class II. The in vitro serial dilution method of antimicrobial screening against *Escherichia coli*, *Staphylococcus aureus*, *Klebsiella aerogenes*, *Pseudomonas aeruginosa*, and *Candida albicans* determined **b3**, **c1**, **c6**, and **c10** as the "lead-compounds" for further modifications to increase the level of activity. Substance **b3** demonstrated antibacterial activity that can be related to the calculated high affinity toward all studied proteins: 50S ribosomal protein L19 (PDB ID: 6WQN), sterol 14-alpha demethylase (PDB ID: 5TZ1), and ras-related protein Rab-9A (PDB ID: 1WMS). The structure–activity and structure–target affinity relationships are discussed. The targets for further investigations and the anatomical therapeutic chemical codes of drug similarity are predicted.

KEYWORDS

5,6-dihydrotetrazolo[1,5-*c*]quinazolines, antimicrobial activity, molecular docking, targets prediction, toxicity prediction

1 | INTRODUCTION

There are known four main principles of antibiotic resistance: treatment with antibiotics, more specifically, through rigorous bacterial diagnosis and resistance testing; to study the origin of resistance and its spread to find ways to neutralize its consequences; to re-examine antibacterial agents that have been shelved by the pharmaceutical industry, possibly due to some level of observed toxicity; and development of novel antimicrobial agents.[1] And the last option was chosen as a promising task for pharmaceutical research to overcome antimicrobial resistance, based on the already discovered activity of structural biologically active analogs.

Tetrazole, as a bioisostere of a carboxylic acid, has the ability to induce various noncovalent interactions such as hydrogen bonds and dipole interactions, which can affect the physicochemical properties,

and the ability to bind to biomolecular targets.[2,3] Its derivatives are resistant to various biological degradation processes, which promote bioavailability,[4,5] and possess various pharmacological properties, such as antimalarial,[2] anti-Alzheimer's,[6] antiangiogenic,[7] anticancer,[8] antihypertensive,[9] and antiviral.[10] Besides, various tetrazole hybrids have been tested for their antibacterial activity, and some of them have shown excellent effects in vitro and in vivo against both drug-susceptible and resistant (including multidrug-resistant) pathogens.[8,11,12] Hence, the modification of their structure by additional antibacterial pharmacophores can increase their activity, and assist in overcoming the drug resistance, by treatment pathogens with the novel substances.

In our previous microbiological screening by disk diffusion method (100 μg/disk) among 2-(1*H*-tetrazolo-5-yl)anilines (10 substances), 1-(2-(1*H*-tetrazolo-5-yl)-R-phenyl)-3-R^1-phenyl(ethyl)ureas (31), *N*-substituted (7) and *S*-substituted tetrazolo[1,5-*c*]quinazole-(6*H*)-5-ones(thiones) (59),[13–15] 21 compounds with antimicrobial activity have been identified (Figure 1).

The strongest activity was demonstrated by 1-(2,5-dimethoxyphenyl)-2-(tetrazolo[1,5-*c*]quinazolin-5-ylthio)ethanone (**1.16**), and 5-(3-chloropropylthio)tetrazolo[1,5-*c*]quinazoline (**1.11**), inhibiting the growth of *C. albicans* at the level of nystatin activity (100 μg/disk). Besides, ethanone **1.16** was almost three times stronger in terms of spectrum and antimicrobial potency, than other substances, still not

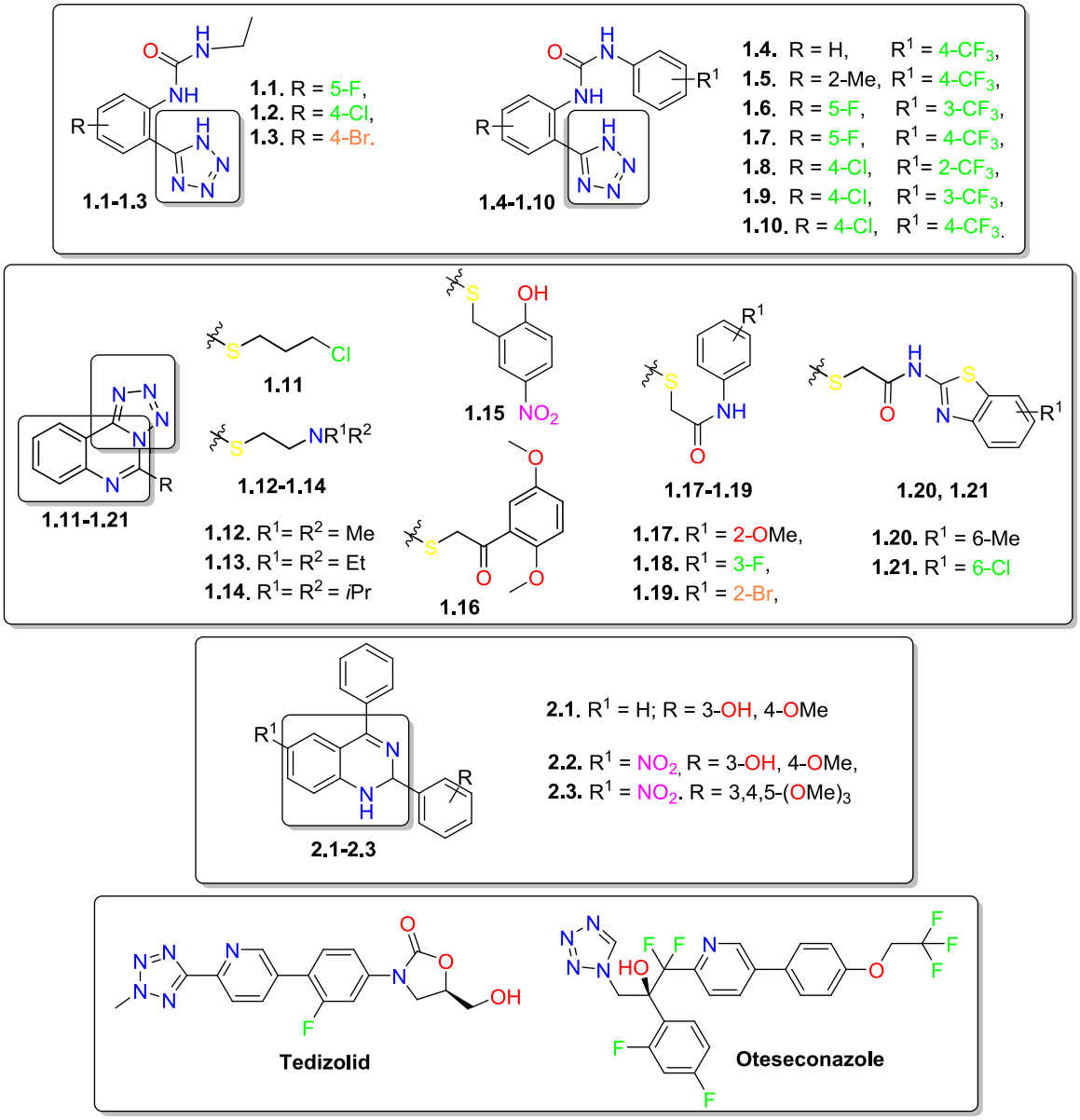

FIGURE 1 The 1-(2-(1*H*-tetrazolo-5-yl)-R-phenyl)-3-R^1-phenyl(ethyl)ureas (**1.1–1.10**) and tetrazolo[1,5-*c*]quinazolines (**1.11–1.21**) with highest demonstrated antimicrobial activity in concentration of 100 μg/disk against *Escherichia coli*, *Staphylococcus aureus*, *Klebsiella aerogenes*, *Klebsiella pneumoniae*, *Enterococcus faecalis*, *Pseudomonas aeruginosa*, and *Candida albicans*. Reference antimicrobial compounds: tedizolid and oteseconazole.

exceeding the antimicrobial level of references like ceftriaxone, gentamycin, and so on. Nevertheless, against each strain, the leading compounds with the best activity were selected, namely: *Staphylococcus aureus* (**1.16**), *Escherichia coli* (**1.1**), *Enterococcus faecalis* (**1.14**), *Pseudomonas aeruginosa* (**1.3**), *Candida albicans* (**1.11, 1.16**), Klebsiella pneumoniae, and *Enterobacter aerogenes* (**1.1**), to form a basis for future structure–activity relationship (SAR) studies.

Moreover, recently, series of 1,2-dihydroquinazoline derivatives were evaluated for their antimicrobial activity using well diffusion method against both Gram-positive bacterial strains such as *Bacillus subtilis*, *S. aureus*, and *Micrococcus luteus*; gram-negative strains such as *Klebsiella planticola*, *E. coli* and *P. aeruginosa*, and fungal strain *C. albicans*.[16] And their minimum inhibition concentation (MIC) values were found in the range of 0.01–0.40 µmol/L, with the most active found substances **2.1–2.3** (Figure 1).

Thus, the synthesis of the condensed analogs of 1*H*-tetrazole and 1,2-dihydroquinazoline is a promising way to obtain novel antimicrobial agents. Besides, the successful design of the active lead compounds for biological and pharmaceutical purposes is accompanied by the molecular docking application,[17] a tool to predict the molecular interactions, which do not depend on molecular descriptors, but relies on a minimum of information from mathematical topological models, and their physico-chemical interpretation. The structure-based drug design is mainly used for binding energy analysis, interaction of ligand-protein and evaluation of the conformational changes during the process of docking.[18–21] It is a method which predicts the preferred orientation of one molecule to a second when a ligand and a target are bound to each other to form a stable complex. And tedizolid and oteseconazole (Figure 1) were chosen as the reference tetrazole containing antimicrobial compounds with an already proven mechanism of desired activity.

Tedizolid[2,22] (torezolid/TR-700, Sivextro, Figure 1) is tetrazole-oxazolidinone antibiotic for the treatment of acute bacterial skin infections caused by certain susceptible bacteria, including *S. aureus* (including methicillin-susceptible and resistant *S. aureus*/MSSA, linezolid-resistant staphylococci), various Streptococcus species (*S. pyogenes*, *S. agalactiae*, *S. anginosus*, *S. intermedius*, and *S. constellatus)*, and *E. faecalis*. It can exert bacteriostatic activity via inhibition of protein synthesis by binding to the 50S ribosomal subunit of the bacteria (bind in the A site of the PTC by interacting with the 23S rRNA component and alters the conformation of a conserved nucleotide in the 23S rRNA (U2585 in *E. coli*), which renders the PTC nonproductive for peptide bond formation).[23] Still, sequence analysis of 23S rRNA, *rrlC* gene and ribosomal protein genes *rplA* and *rspQ*, performed on the recovered WIS 423 tedizolid-mutant strain, revealed that this strain possessed the G2576T mutation in one of the six copies of 23S rRNA,[24] which could lead to reduced tedizolid susceptibility.

Oteseconazole (VT-1161 or SHR8008 in China) (Figure 1), a tetrazole-pyridine hybrid, is an oral selective inhibitor of fungal CYP51 (14-alpha demethylase, that participates in the formation of ergosterol, a compound that plays a vital role in the integrity of cell membranes), designed to treat recurrent vulvovaginal candidiasis without off-target toxicities.[25] And it has a strong potential in the fight against other fungal infections, including azole-resistant, as it has a tetrazole moiety, that improved its target selectivity due to the attenuated interaction between the metal-binding groups and the heme cofactor.[26] Also, it has a better selectivity for fungal CYP51 polypeptide, than can be seen with other azole drugs, with less interaction with off-target human cytochrome P450s, thus reducing the potential for safety issues.[27]

Considering the abovementioned data of reference compounds, the following proteins were chosen as the targets for conduction of in silico molecular docking in this study: (1) 50S ribosomal protein L19 of the ribosome from methicillin resistant *S. aureus* (PDB ID: 6WQN),[28] because antibacterial activity of tedizolid is mediated by binding to the 50S subunit of the bacterial ribosome, resulting in the inhibition of protein synthesis;[23] and (2) sterol 14-alpha demethylase (PDB ID: 5TZ1)[29] from *C. albicans*, as it is known that azoles as well as oteseconazole, inhibit the activity of fungal cytochrome P450 (CYP) enzyme 51 (CYP51) via competitive and reversible binding to the heme cofactor in the enzyme active site,[30,31] and (3) ras-related protein human Rab9 GTPase: (PDB ID: 1WMS),[32] because according to Super-PRED target prediction website.[33], it is assigned to Fungal infection [ICD-11: 1F29-1F2F] treatment by International Classification of Diseases-11 (ICD-11); it is involved in the transport of proteins between the endosomes and the trans-Golgi network; in the recruitment of SGSM2 to melanosomes and is required for the proper trafficking of melanogenic enzymes TYR, TYRP1, and DCT/TYRP2 to melanosomes in melanocyte,[34] and also recently been found to be a key cellular component for human immunodeficiency virus-1, Ebola, Marburg, and measles virus replication,[32] so is additionally an interesting antiviral drug target for widening the spectrum of substances' possible application.

Hence, herein we present the synthesis and structure evaluation of 18 novel 5,6-dihydrotetrazolo[1,5-*c*]quinazolines; predict their toxicity level; investigate in vitro antimicrobial minimum inhibition concentration (MIC) by broth tube dilution method[35] against *S. aureus*, *E. coli*, *P. aeruginosa*, *K. pneumonia*, and *C. albicans*; conduct the molecular docking to propose the activity mechanism; discuss SAR, and consider the future directions of their investigation by prediction the other protein targets, and anatomical therapeutic chemical (ATC) codes of drug similarity.

2 | RESULTS AND DISCUSSION

2.1 | Toxicity prediction

So, it was decided to enhance antimicrobial activity level of the abovementioned tetrazolo[1,5-*c*]quinazoline derivatives (Figure 1) by modification them into the novel 5,6-dihydrotetrazolo[1,5-*c*]quinazolines bearing cycloalkyl, aryl, heteroaryl fragments with alkyl, halogen, hydroxy, cyano and carboxylic acid substituents (Scheme 1), which are among the most frequently occurring groups in bioactive molecules described in medicinal chemistry literature.[36]

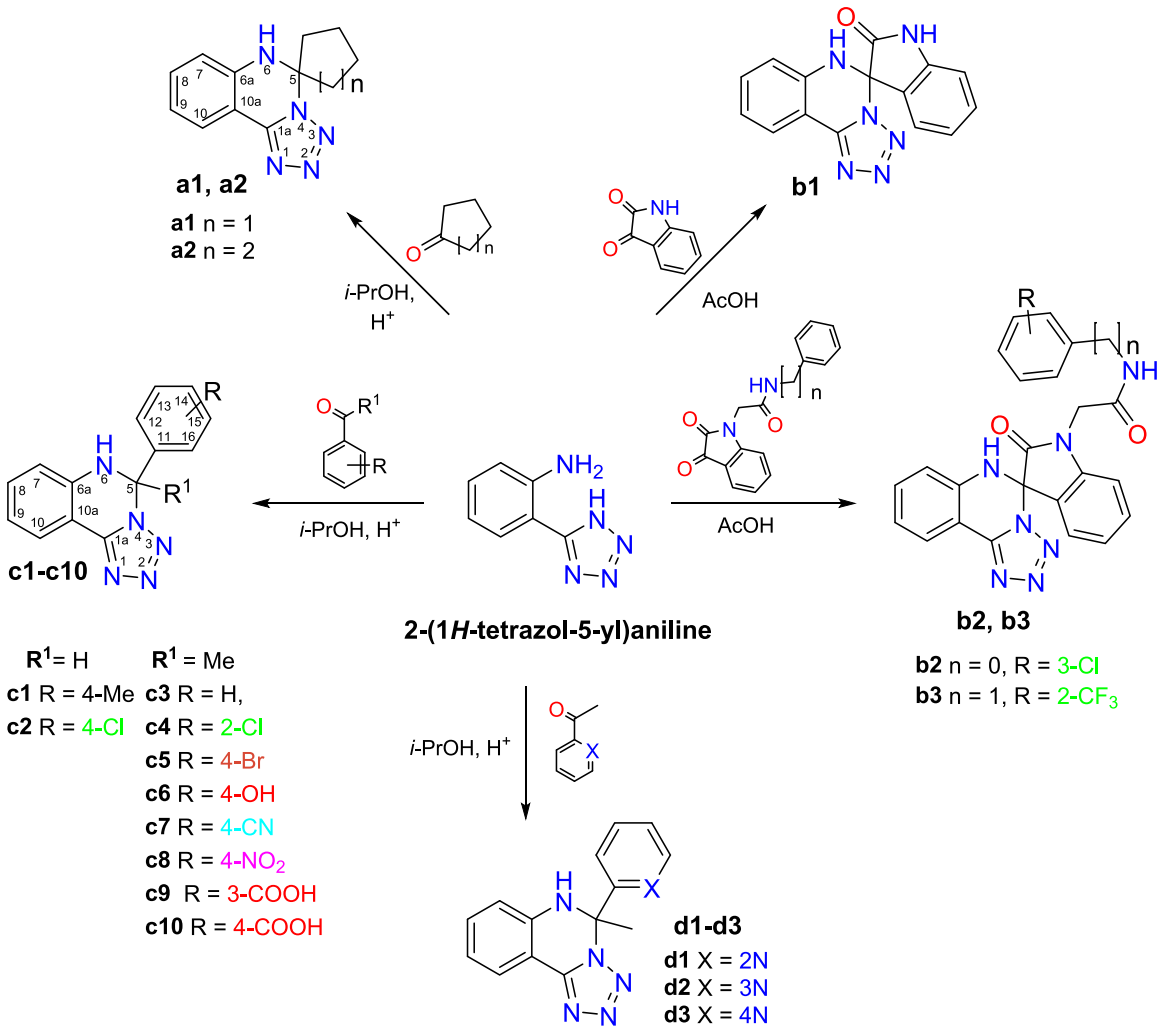

SCHEME 1 Synthesis of the 5,6-dihydrotetrazolo[1,5-*c*]quinazolines.

To our knowledge 5,6-dihydrotetrazolo[1,5-*c*]quinazoline derivatives are practically not reported in the literature. There were shown only a few examples, namely molecular structure of **a1**[37] (Scheme 1); cyclisation of quinazolines with azides to obtain **a1**[38] and **a2**;[39] crystallographic data of 8-chloro-5,5-dimethyl[40] derivatives; and synthesis of nine 9-methyl/methoxy-5-methyl-5-phenyl/hexyl/ethylphenyl/-5,6-dihydrotetrazolo[1,5-*c*]quinazolines by $Ph_3PAuOTf$-catalyzed direct double hydroamination of alkynes.[41] In the Drugbank,[42] there are found only 24 approved drugs containing 1*H*-tautomer of tetrazole, 30 experimental compounds, and only 4 experimental 1,2-dihydroquinazolines, but their condensed derivatives are not found in this base. So, the derivatization into fused functional derivatives is an interesting and promising task from a pharmaceutical point of view.

Moreover, before synthesis, computational toxicity estimation can help to reduce the amount of animal experiments, as well it makes the determination of toxic doses faster. The online website ProTox-II[43,44] was used for prediction of the toxicity indexes (Table 1), that were defined according to the globally harmonized system of classification of chemicals (GHS) labeling.

As it is seen from the Table 1, the predicted hepatotoxicity, carcinogenicity and mutagenicity for the majority of the substances is of low level. So, they were predicted to be of toxicity Class V: may be harmful if swallowed ($2000 < LD_{50} \leq 5000$). Still, the strong toxicity was found for the series **b**, but at least without hepatotoxicity warning. The **b3** was calculated to be of Class II: fatal if swallowed ($5 < LD_{50} \leq 50$). Considering the toxicity level of known nonsteroidal anti-inflammatory drug celecoxib,[45] that contains CF_3 group too, it was found of IV Class, but with LD_{50} lower than of **b3**. Moreover, for this drug Estrogen Receptor Alpha (ER) toxicity prediction was 1 of 1. Moreover, for another drug with CF_3 group, namely, the antidepressant fluoxetine,[46] it was calculated with even 100% probability to be Class III: toxic if swallowed ($50 < LD_{50} \leq 300$). The other two representatives of spiro-indoline derivatives **b1** and **b2**, were of Class IV: harmful if swallowed ($300 < LD_{50} \leq 2000$). And, due to the presence of nitro group in the molecule of **c8**, it has the highest carcinogenicity and mutagenicity predicted. It worth to mention, that despite the shown 71% of immunotoxicity and hepatotoxicity for reference antifungal oteseconazole, it was approved by FDA.[47] And with other antimicrobial agent tedizolid, they are of toxicity Class IV with LD_{50} of 1000–1500 mg/kg.

TABLE 1 The prediction of substances' toxicity.

#	Oral toxicity			Prediction: active, probability from 1[a]				
	Toxicity index	LD_{50} (mg/kg)	Prediction accuracy (%)	Hepatotoxicity	Carcinogenicity	Mutagenicity	MMP[b]	Aromatase/AhR[b]
CB[c]	4	1400	54.26	–	0.56	–	–	–
FT	3	248	100.00	–	–	–	–	–
O	4	1500	67.38	0.61	–	0.50	–	–
T	4	1000	54.26	0.71	–	–	–	–
b1	4	2000	23.00	0.60	0.59	–	–	–
b2	4	1000	54.26	–	–	0.56	–	–
b3	2	2000		–	0.52	0.54	–	–
a1	5	2500		–	0.52	0.57	–	–
a2				–	0.51	0.57	–	–
c1				0.55	0.53	0.51	–	–
c2				0.52	–	–	–	0.50/no
c3				0.54	0.53	–	–	
c4				0.52	–	–	–	0.53/no
c5				0.56	–	–	–	–
c6				0.59	0.51	–	–	no/0.50
c7				0.54	0.51	–	–	–
c8				0.59	0.82	0.84	0.63	–
c9				0.62	0.53	–	–	–
c10				0.62	0.53	–	–	–
d1				0.54	0.53	–	–	–
d2				0.54	0.53	–	–	–
d3				0.54	0.53	–	–	–

[a]Toxicity model report illustrates the confidence of positive toxicity results compared to the average of its class in hepatotoxicity, carcinogenicity, immunotoxicity, mutagenicity, cytotoxicity.

[b]AhR, aryl hydrocarbon receptor; AR, androgen receptor; AR-LBD, androgen receptor ligand binding domain; ATAD5, ATPase family AAA domain-containing protein 5; ER, aromatase, estrogen receptor alpha; ER-LBD, estrogen receptor ligand binding domain; HSE, heat shock factor response element phosphoprotein (tumor suppressor) p53; MMP, mitochondrial membrane potential; nrf2/ARE, nuclear factor (erythroid-derived 2)-like 2/antioxidant responsive element; PPAR-gamma, peroxisome proliferator activated receptor gamma.

[c]CB, celecoxib: additionally, estrogen receptor alpha (ER) is predicted of 1; FT, fluoxetine; O, oteseconazole: additionally immunotoxicity is predicted of 0.71; T, tedizolid.

So, the results of the toxicity prediction of majority of the novel synthesized compounds are promising, nevertheless, to make the definite conclusion of their toxic properties the in vitro and in vivo experiments should be done.

2.2 | Synthesis

The novel 5,6-dihydrotetrazolo[1,5-*c*]quinazolines (**a–d**) (Scheme 1) were obtained by reaction of cycloaddition of 2-(1*H*-tetrazol-5-yl) aniline as binucleophile with corresponding aldehydes or ketones.[48] The LC-MS and the elemental analysis confirmed the structure, and the purity of the obtained compounds. In ^{13}C NMR spectra, the carbon signal of C5 was observed in the region 77.35–71.18 ppm; all other signals are assigned in the Experimental part. In the ^{1}H NMR spectra of 6′*H*-spiro[cycloalkyl-1,5′-tetrazolo[1,5-*c*]quinazolines **a1** and **a2**, the signal of quinazoline NH was found at the 7.25–7.07 ppm, the H7-H10 protons of aromatic ring were presented at the 7.79–6.69 ppm, and the cycloalkyl ring at the 2.38–1.47 ppm. For 6′*H*-spiro(indoline-3,5′-tetrazolo[1,5-*c*]quinazolines) **b1–b3**, the protons of the aromatic ring were registered at the 7.89–6.83 ppm; indole NH was observed as a singlet at the 10.77 ppm; acetamide NH of **b2** and **b3** was found at the 10.48–8.77 ppm, and quinazoline NH at the 8.01–8.18 ppm. The series of 5,6-dihydrotetrazolo[1,5-*c*]quinazolines **c** were evaluated by the signals of quinazoline NH at the 8.26–7.65 ppm; protons of an aromatic ring at the 7.83–6.62, and alkyl substituents at the 2.36–2.24 ppm. For benzoic acid derivatives **c9** and **c10**, singlets of COOH were registered at the 12.78 and 12.65

ppm. Considering series of 5-(pyridinyl)-5,6-dihydrotetrazolo[1,5-*c*]quinazoline **d**, protons of pyridinyl core and quinazoline ring were partially overlapped, and were found at 8.58–6.82 ppm. Their NH were registered as singlets at the 8.33–8.01 ppm; and methyl protons at the 2.33–2.32 ppm. In the IR spectra, the characteristic peaks of functional groups corresponded to the proposed structure (Supporting Information Figures).

2.3 | Molecular docking

In the result of the in silico molecular docking studies, the following affinities were found between 18 compounds and two references toward mentioned above 50S ribosomal protein L19 (PDB ID: 6WQN),[28] sterol 14-alpha demethylase (PDB ID: 5TZ1),[29] and ras-related protein Rab-9A (PDB ID: 1WMS)[32] (Table 2).

The substances **b3** and **b2** have shown the strongest affinity toward all enzymes. And even against sterol 14-alpha demethylase (PDB ID: 5TZ1), **b3** had better result than oteseconazole. On the other hand, unsubstituted **a1** (6′*H*-spiro[cyclopentane-1,5′-tetrazolo[1,5-*c*]quinazoline]), **c2** (5-(4-chlorophenyl)-5,6-dihydrotetrazolo[1,5-*c*]quinazoline), and **d** series of 5-methyl-5-(pyridinyl)-5,6-dihydrotetrazolo[1,5-*c*]quinazolines had the least favorable structures for studies proteins. All calculated bonds and interactions toward the amino acid residues can be found in the Supporting Information: Tables S2–S4.

In the 3D representation (Figure 2), it is nicely seen how **b3** effectively fits into the active pockets of the enzymes due to flexibility of its structure. In correlation to the found affinity, the fewest number of bonds were formed by **b3** toward 50S ribosomal protein L19, and the highest—to sterol 14-alpha demethylase (Supporting Information: Tables S2–S4). Interesting, that in each case, different amino acids residues were taken part in the bond's formation. And the electrostatic π-cation bond and hydrophobic π–π shaped were formed only toward ras-related protein Rab-9A.

Hence, due to the predicted affinity toward antimicrobial targets, such activity was expected to be found during in vitro experiments.

2.4 | Antimicrobial studies

So, the next step of the study was in vitro serial dilution method[35] of antimicrobial screening against *E. coli*, *S. aureus*,

TABLE 2 Affinity of investigated substances toward to binding sites of 50S ribosomal protein L19 (PDB ID: 6WQN), sterol 14-alpha demethylase (PDB ID: 5TZ1), ras-related protein Rab-9A (PDB ID: 1WMS), kcal/mol.

Substance	50S ribosomal protein L19 (kcal/mol)	Substance	Sterol 14-alpha demethylase (kcal/mol)	Substance	Ras-related protein Rab-9A (kcal/mol)
b2	−9.7	**b3**	−10.9	**b3**	−8.4
b3	−9.6	Oteseconazole	−10.4	**b2**	−8.3
b1	−9.0	**b2**	−10.2	**c8**	−8.0
c8	−8.5	Tedizolid	−9.3	**c6**	−8.0
c4	−8.5	**c7**	−9.0	**c9**	−7.9
c10	−8.2	**c10**	−8.8	**c7**	−7.9
c9	−8.1	**c5**	−8.8	**c10**	−7.8
c6	−7.9	**c9**	−8.8	**c5**	−7.7
d1	−7.9	**b1**	−8.7	**b1**	−7.6
d2	−7.8	**c1**	−8.6	**a2**	−7.6
d3	−7.8	**c2**	−8.5	**c4**	−7.6
c7	−7.8	**c4**	−8.3	**c1**	−7.6
c5	−7.7	**c8**	−8.3	**c3**	−7.4
c3	−7.7	**c3**	−8.2	**d1**	−7.4
c1	−7.4	**c6**	−8.2	**d2**	−7.4
a2	−7.3	**a2**	−7.9	**d3**	−7.4
c2	−7.3	**d1**	−7.9	**c2**	−7.3
Tedizolid	−7.2	**d2**	−7.8	**a1**	−7.2
Oteseconazole	−7.1	**d3**	−7.6	Oteseconazole	−6.7
a1	−7.0	**a1**	−7.5	Tedizolid	−5.6

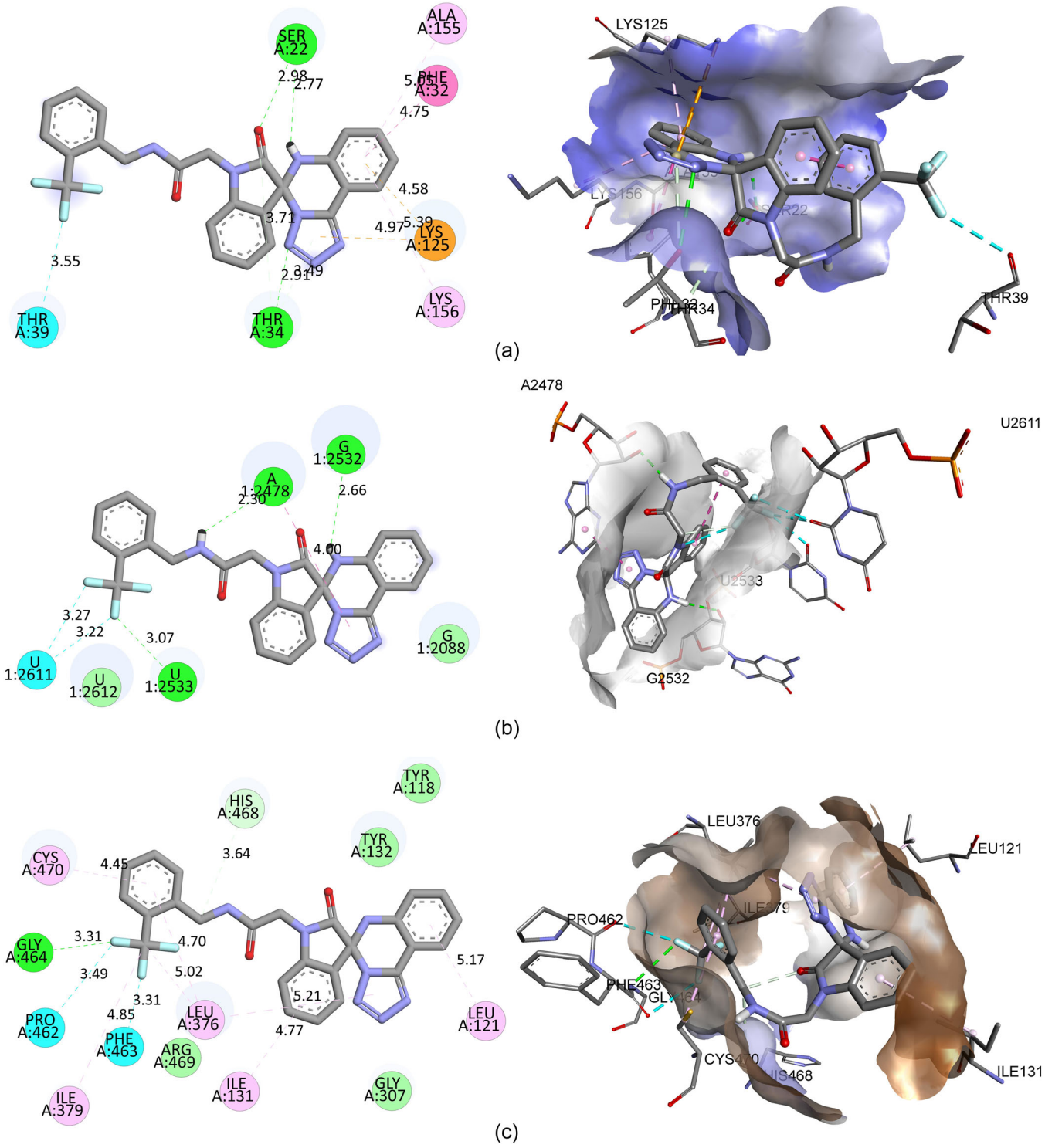

FIGURE 2 Visual representation (2D and 3D) of the lead compound **b3** showing bonds formation indicated in Å in the active site of ras-related protein Rab-9A (PDB ID: 1WMS). (**a**) 50S ribosomal protein L19 (PDB ID: 6WQN) (**b**), and sterol 14-alpha demethylase (PDB ID: 5TZ1). (**c**) Green—conventional hydrogen bond; pale green—carbon hydrogen, or π donor hydrogen bonds, or van der Waals interaction; blue—halogen (fluorine); orange—electrostatic π-cation; magenta—hydrophobic π–π stacked, or π–π T shaped; rose—π-alkyl, or alkyl bonds.

K. aerogenes, *P. aeruginosa*, and *C. albicans* among all 18 tested compounds. *P. aeruginosa* and *K. aerogenes* appeared to be insensitive to all synthesized series of 5,6-dihydrotetrazolo[1,5-*c*] quinazolines. And only 6 compounds (**b3**, **c1**, **c6**, **c9**, **c10**, and **d1**) demonstrated antifungal and different antibacterial activities (Table 3).

The promising preliminary antimicrobial activity of **c10** against *S. aureus* was reported by us earlier.[49] Summing up the

TABLE 3 Antimicrobial activity results of serial dilution method.

Strain	Active substance	Absence (−)/presence (+) of opalescence in test tube Concentration (2–256, mg/L)/active substance (mM)							
		256	128	64	32	16	8	4	2
Staphylococcus aureus	**b3**	−/0.51	−/0.25	+	+	+	+	+	+
	c10	−/0.83	−/0.41	−/0.21	−/0.11	+	+	+	+
Escherichia coli	**c10**	−/0.83	+	+	+	+	+	+	+
Candida albicans	**c1**	−/0.97	−/0.48	+	+	+	+	+	+
	c6	−/0.92	−/0.46	+	+	+	+	+	+
	c9	−/0.83	+	+	+	+	+	+	+
	c10	−/0.83	+	+	+	+	+	+	+
	d1	−/0.97	+	+	+	+	+	+	+
Pseudomonas aeruginosa, *Klebsiella aerogenes*	All	+	+	+	+	+	+	+	+
Growth control	All	+	+	+	+	+	+	+	+
Sterility control	All	–	–	–	–	–	–	–	–

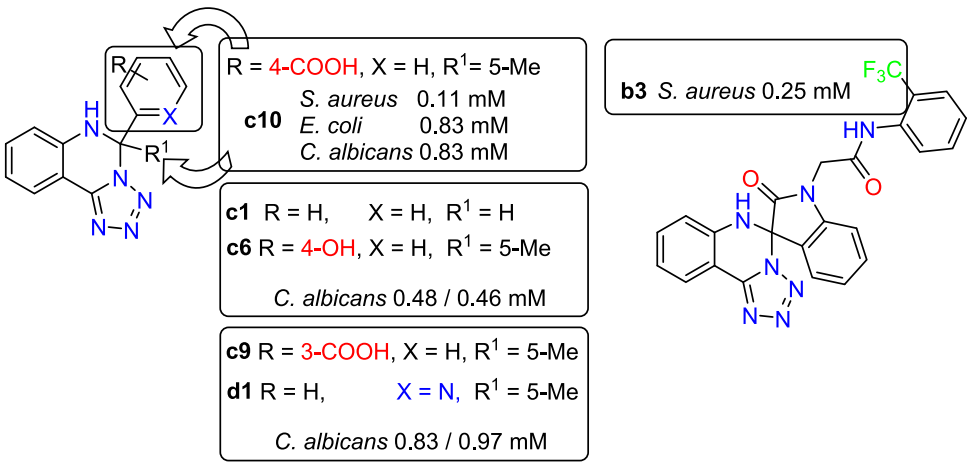

FIGURE 3 Structure–antimicrobial activity relationship and minimum inhibition concentation (mM) of active compounds.

found MIC results and the SAR in the Figure 3, it is shown that the incorporation of the carboxylic groups into the 4th position of the phenyl substituent lead to the manifestation of the antibacterial activity of **c10** against *S. aureus*, *E. coli*, and antifungal against *C. albicans*. Interesting that **c9**, bearing also COOH, but in the 3rd position, had only the same weak antifungal properties against *C. albicans* with an MIC of 0.83 mM, but had no antibacterial activity.

The presence of 4-OH group in the phenyl ring of **c6** had the same effect for antifungal activity presence as 5-methyl in the 5,6-dihydrotetrazolo[1,5-*c*]quinazoline core of **c1** with 128 mg/L (0.48/0.46 mM, respectively). And interesting, that only one pyrimidin-2-yl substituent present in **d1**, among all three different isomers of **d** series promoted the antifungal properties. Besides, the presence of 2-trifluoromethyl group in the 2-(2-oxoindolin-1-yl)-*N*-(2-(trifluoromethyl)phenyl)acetamide fragment of **b3** has made it active against *S. aureus* with MIC of 0.25 mM.

So, due to the high predicted affinity (−9.6 kcal/mol) toward 50S ribosomal protein L19 (PDB ID: 6WQN)[28] of substance **b3**, its mechanism of its antibacterial activity against *S. aureus* could be due to inhibition of protein synthesis by binding to the 50S ribosomal subunit of the bacteria,[23] which additionally should be tested in vitro. Antifungal mechanism of the studied series of compounds is also expected to be of sterol 14-alpha demethylase[29] inhibition, but detected MICs had weaker correlation to above found affinities to the enzyme.

Nevertheless, the above-mentioned scaffolds were chosen as the most promising ones for the future modifications with the aim to obtain the novel antimicrobial substances to overcome antimicrobial resistance. Besides, fluconazole is reported to have MIC against *C.*

albicans ≤0.125 mg/L and oteseconazole even ≤0.03 mg/L,[25] so their activity level should be increased.

2.5 | Targets prediction

Considering the low predicted toxicity of the majority of the novel substances (Table 1), it was decided to analyze the additional directions of biological activity studies, because except the mentioned earlier pharmacological properties of tetrazole bearing representatives,[2–15] in 1974 year 5,6-dihydrotetrazolo[1,5-*c*]quinazoline derivatives were reported to be the bronchodilator agents.[37] Also, 1*H*-tetrazole bearing olmesartan[50] belongs to the angiotensin II receptor blocker (ARB) family of drugs, which also includes telmisartan, candesartan, losartan, valsartan, and irbesartan, which selectively binds to angiotensin receptor 1 (AT1) and prevents the protein angiotensin II from binding and exerting its hypertensive effects, which include vasoconstriction, stimulation and synthesis of aldosterone and ADH, cardiac stimulation, and renal reabsorption of sodium, among others. Thus, results of the prediction of other possible targets for studied compounds were expected to be versatile.

The webserver Super-PRED[51] was used for targets and ATC codes[33] prediction. And, it's worth to mention, that the predicted ras-related protein Rab-9A inhibition by **c9** and **c10** was potentially confirmed by their *in vitro* antifungal activity (Table 3, Figure 4). Nevertheless, it should be proved by its direct inhibition.

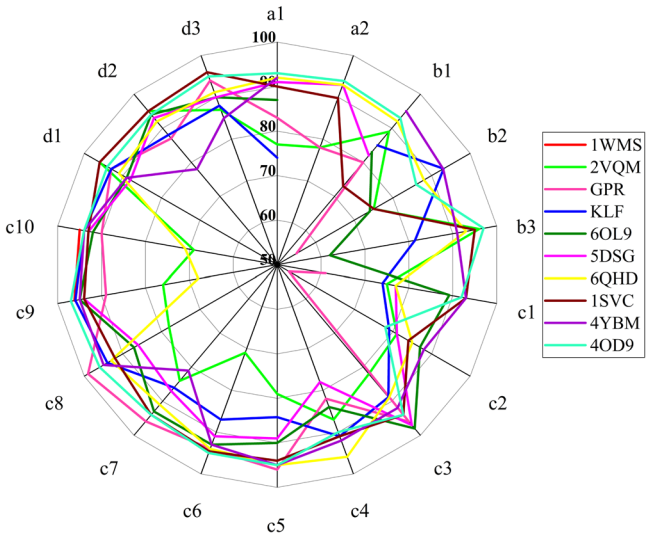

FIGURE 4 The calculated probability (%) toward targets (PDB ID): Ras-related protein Rab-9A: 1WMS; muscarinic acetylcholine receptor M4: 5DSG; G-protein coupled receptor 55: GPR, PDB ID is not available; Kruppel-like factor 5: KLF, PDB ID is not available; histone deacetylase 4: 2VQM; muscarinic acetylcholine receptor M5: 6OL9; signal transducer and activator of transcription 3: 6QHD; nuclear factor NF-kappa-B p105 subunit: 1SVC;. transcription intermediary factor 1-alpha: 4YBM; cathepsin D: 4OD9. The average probability toward targets for all 18 substances is increasing from 1WMS to 4OD9.

Thus, cathepsin D was found as the target with the highest average probability of 93% to have affinity toward all series of compounds, associated with multiple sclerosis and hypertension (Table 4, Figure 4, Supporting Information: Table S5). The results of substances **c9** and **c10** (due to the calculated additional affinities toward Ras-related protein Rab-9A), and for **c3**, **c5**, **c7**, **c8**, and **d1–d3** appeared to have the widest range of predicted targets. And the highest affinity probability of 99% was found for **c8** toward G-protein coupled receptor 55, and of 98% for **c3** against muscarinic acetylcholine receptor M5 (Supporting Information: Table S5).

Moreover, according to the proposed targets names, there are shown the variety of the ICD-11 to be treated (Table 4).[33]

And, finally, various ATC codes of drug similarity are presented in Table 5.

Thus, substance **c8** has the highest certainty (64.16%) among all studied compounds to be among of N05CD series: benzodiazepine derivative hypnotics and sedatives. Substances of **b** series, **b2** and **b3**, **d2** and the active substance **c10** demonstrated the widest range of ATC codes (Table 5). Nevertheless, the prior analysis[52] of PAINS (pan assay interference compounds, a.k.a. frequent hitters or promiscuous compounds)[53] has detected no alert for substance **c10** to be a molecule containing substructures showing potent response in assays irrespective of the protein targets. Considering substances **c6** and **b1**, they could be investigated to be of A06AB: contact laxatives also with good probability. And interesting that only **c7** was predicted to be among on-nucleoside reverse transcriptase inhibitors with 23.33% probability.

3 | CONCLUSION

A series of novel 5,6-dihydrotetrazolo[1,5-*c*]quinazolines were synthesized. Their structure was elucidated by NMR, IR and LC-MS spectra. The majority of the substances were predicted to have the toxicity of the Class V. The antimicrobial study by the broth dilution method has found six substances possessing antifungal and antibacterial properties, among which substance **c10** has the widest range of activities. The strongest activity against *S. aureus* was demonstrated by the latter (0.11 mM), and against *C. albicans* by **c1** (0.48 mM) and **c6** (0.46 mM). The SAR illustrated the impact for antibacterial activity demonstration of not only carboxylic group presence in molecule, but its exact position in the molecule (4th for **c10** *vs*. 3rd for **c9**). Although for antifungal activity against *C. albicans* it had no difference. The molecular docking results demonstrated that **b3** and **b2** had the highest affinity toward all studied proteins, showing promising results to be studied against other antimicrobial strains along with active **c1**, **c6**, and **c10**. Additionally, 10 targets with high probability up to 95%–99% affinity toward synthesized series of compounds are proposed for future research to show more strong results, along with their ICD-11 indication, and ACT classification of drug similarity.

TABLE 4 The international classification of diseases-11 (ICD-11) indications according to the predicted targets.

Target name[a]	ICD-11 indication	
Ras-related protein Rab-9A	Fungal infection [ICD-11: 1F29-1F2F]	
Muscarinic acetylcholine receptor M4	Asthma [ICD-11: CA23]	Glaucoma/ocular hypertension [ICD-11: 9C61]
	Attention deficit hyperactivity disorder [ICD-11: 6A05.Z]	Mydriasis [ICD-11: LA11.62]
	Bronchial hyperreactivity [ICD-11: CB40]	Nausea [ICD-11: MD90]
G-protein coupled receptor 55	Attention deficit hyperactivity disorder [ICD-11: 6A05.Z]	
Histone deacetylase 4	Advanced stage follicular lymphoma [ICD-11: 2A80]	Solid tumor/cancer [ICD-11: 2A00-2F9Z]
	Huntington disease [ICD-11: 8A01.10]	
Muscarinic acetylcholine receptor M5	Acquired nystagmus [ICD-11: 9C84]	Hypertension [ICD-11: BA00-BA04]
	Allergic rhinitis [ICD-11: CA08.0]	Irritable bowel syndrome [ICD-11: DD91.0]
	Alzheimer disease [ICD-11: 8A20]	Myasthenia gravis [ICD-11: 8C6Y]
	Amnesia [ICD-11: MB21.1]	Neurological disorder [ICD-11: 6B60]
	Asthma [ICD-11: CA23]	Nocturia [ICD-11: MF55]
	Attention deficit hyperactivity disorder [ICD-11: 6A05.Z]	Organophosphate poisoning [ICD-11: NE6Z]
	Brain disease [ICD-11: 8C70-8E61]	Overactive bladder [ICD-11: GC50.0]
	Central and peripheral nervous disease [ICD-11: 8A04-8E7Z]	Pancreatitis [ICD-11: DC31-DC34]
	Chronic obstructive pulmonary disease [ICD-11: CA22]	Parkinson disease [ICD-11: 8A00.0]
	Cognitive impairment [ICD-11: 6D71]	Peptic ulcer [ICD-11: DA61]
	Colitis [ICD-11: 1A40.Z]	Psychomotor agitation [ICD-11: MB23.M]
	Cough [ICD-11: MD12]	Schizophrenia [ICD-11: 6A20]
	Depression [ICD-11: 6A70-6A7Z]	Solid tumor/cancer [ICD-11: 2A00-2F9Z]
	Dysmenorrhea [ICD-11: GA34.3]	Spasm [ICD-11: MB47.3]
	Dysuria [ICD-11: MF50.7]	Stomach ulcer [ICD-11: DA60.Z]
	Examination of eyes or vision [ICD-11: QA00.6]	Suprapubic pain [ICD-11: MG30-MG3Z]
	Gastric motility disorder [ICD-11: DA21]	Urgency [ICD-11: N.A.]
	Gastritis [ICD-11: DA42]	Urinary incontinence [ICD-11: MF50.2]
	Gastrointestinal disease [ICD-11: DE2Z]	Urinary retention [ICD-11: MF50.3]
	Glaucoma/ocular hypertension [ICD-11: 9C61]	Uveitis [ICD-11: 9A96.Z]
Signal transducer and activator of transcription 3	Brain cancer [ICD-11: 2A00]	Multiple myeloma [ICD-11: 2A83]
	Chronic lymphocytic leukemia [ICD-11: 2A82.0]	Psoriasis vulgaris [ICD-11: EA90]
	Hepatocellular carcinoma [ICD-11: 2C12.02]	Recurrent glioblastoma [ICD-11: 2A00.00]
	Immune System disease [ICD-11: 4A01-4B41]	Solid tumor/cancer [ICD-11: 2A00-2F9Z]
	Inflammation [ICD-11: 1A00-CA43.1]	Ulcerative colitis [ICD-11: DD71]
Cathepsin D	Hypertension [ICD-11: BA00-BA04]	Multiple sclerosis [ICD-11: 8A40].

[a]Kruppel-like factor 5, transcription intermediary factor 1-alpha, nuclear factor NF-kappa-B p105 subunit: there were no indications.

4 | EXPERIMENTAL

4.1 | Toxicity studies

A virtual lab of website ProTox-II was used for the prediction toxicities of molecules.[43,44] It incorporates molecular similarity, fragment propensities, most frequent features and (fragment similarity-based CLUSTER cross-validation) machine-learning, based on a total of 33 models for the prediction of various toxicity endpoints such as acute toxicity, hepatotoxicity, cytotoxicity, carcinogenicity, mutagenicity, immunotoxicity, adverse outcomes (Tox21) pathways and toxicity targets. All methods, statistics of

TABLE 5 Drug classification with selection of the highest predicted certainty for the studied compounds.

#	ATC code	%	ATC code	%	ATC code	%	ATC code	%
c8	N05CD	64.16						
c6	A06AB	40.82						
b1	A06AB	31.28						
c3	N03AB	26.58						
c7	J05AG	23.33	N03AB	6.47				
c9	N03AB	16.25						
d2	R07AB	15.96	N03AB	10.29	A02BC	7.08		
b2	N05BA	14.76	N06AA	12.59	R03DC	9.62	N05CD	5.86
b3	N06AA	11.67	N03AB	9.11	R03DC	6.93	L02BB	5.84
a2	N06AA	9.19	R07AB	6.18				
c5	N05CD	9.16	N03AB	6.39				
c4	N05CD	9.11						
a1	N06AA	8.99	N03AB	5.03				
d3	C01CE	8.49	N03AB	6.09				
c2	N05BA	8.16	B01AA	7.87				
c1	N03AB	7.58	N06AA	6.47				
c10	A06AB	6.50	N03AB	6.33	C09CA	6.15	B02AA	5.62

Note: N05CD: Benzodiazepine derivative hypnotics and sedatives; A06AB: Contact laxatives; J05AG: on-nucleoside reverse transcriptase inhibitors; N03AB: Hydantoin derivatives, antiepileptics; R07AB: Respiratory stimulants; A02BC: Proton pump inhibitors for peptic ulcer and GORD; N05BA: Benzodiazepine derivative anxiolytics; N06AA: Nonselective monoamine reuptake inhibitors/antidepressants; R03DC: Leukotriene receptor antagonists for obstructive airway diseases; L02BB: Anti-androgen hormone antagonists and related agents; C01CE: Phosphodiesterase inhibitors, cardiac; B01AA: Vitamin K antagonists/antithrombotic; C09CA: Angiotensin II receptor blockers (ARBs), plain; B02AA: Antifibrinolytic amino acids.

training set as well as the cross-validation results can be found at their website. Toxicity Model Report illustrates the confidence of positive toxicity results compared to the average of its class in hepatotoxicity, carcinogenicity, immunotoxicity, mutagenicity, cytotoxicity, Aryl hydrocarbon receptor (AhR), androgen receptor (AR), androgen receptor ligand binding domain (AR-LBD), aromatase, estrogen receptor alpha (ER), estrogen receptor ligand binding domain (ER-LBD), peroxisome proliferator activated receptor gamma (PPAR-gamma), nuclear factor (erythroid-derived 2)-like 2/antioxidant responsive element (nrf2/ARE), Heat shock factor response element (HSE), mitochondrial membrane potential (MMP), phosphoprotein (tumor suppressor) p53, ATPase family AAA domain-containing protein 5 (ATAD5).

4.2 | Synthesis

4.2.1 | General remarks

Melting points were determined in open capillary tubes in a «Mettler Toledo MP 50» apparatus and were uncorrected. The elemental analyses (C, H, N) were performed using the ELEMENTAR vario EL cube analyzer. Analyses were indicated by symbols of the elements or functions within ±0.3% of the theoretical values. ^{1}H NMR spectra (400 MHz) and ^{13}C NMR spectra (125 MHz) were recorded on a Varian-Mercury 400 (Varian Inc.) spectrometers with TMS as internal standard in DMSO-d_6 solution. LC-MS were recorded using chromatography/mass spectrometric system which consists of high-performance liquid chromatography «Agilent 1100 Series» (Agilent) equipped with diode-matrix and mass-selective detector «Agilent LC/MSD SL» (atmospheric pressure chemical ionization [APCI]). Electron impact mass spectra (EI-MS) were recorded on a Varian 1200 L instrument at 70 eV (Varian). The purity of all obtained compounds was checked by ^{1}H-NMR and LC-MS.

The InChI codes of the investigated compounds, together with some biological activity data, are provided as Supporting Information.

4.2.2 | General procedure for the synthesis of 5, 6-dihydrotetrazolo[1,5-*c*]quinazolines

2-(1*H*-Tetrazol-5-yl)aniline (1.0 g; 6 mM) was dissolved in propan-2-ol (10 mL) or acetic acid (compounds **b1–b3**). Then,Then, the corresponding aldehyde or ketone (6 mM) was added to the solution. In

case when propan-2-ol was used as a solvent, one drop of concentrated sulfuric acid was added. The mixture was refluxed for 1 h. and cooled. A formed precipitate was filtered and washed first with propan-2-ol (5 mL), then with cold water (100 mL).

*6′H-Spiro[cyclopentane-1,5′-tetrazolo[1,5-c]quinazoline] (**a1**)*

Beige solid in 51.10% yield, mp 167–169°C. ^{1}H NMR (400 MHz): δ (ppm): 7.79 (d, *J* = 7.7 Hz, 1H, H-10), 7.29 (t, *J* = 7.8 Hz, 1H, H-8), 7.25 (s, 1H, NH), 6.91 (d, *J* = 8.2 Hz, 1H, H-7), 6.85 (t, *J* = 7.5 Hz, 1H, H-9), 2.38 (dt, *J* = 13.7, 7.1 Hz, 2H, CH_2CH_2), 2.12 (dd, *J* = 14.0, 7.0 Hz, 2H, CH_2CH_2), 1.94 (td, *J* = 8.6, 7.4, 4.9 Hz, 4H, CH_2CH_2, CH_2CH_2). IR (cm^{-1}): 1621, 1481, 1315, 775, 747, 689. LC-MS: *m/z* = 228 $[M+H]^+$. Anal. calcd. for $C_{12}H_{13}N_5$: C, 63.42; H, 5.77; N, 30.82. Found: C, 63.47; H, 5.71; N, 30.88.

*6′H-Spiro[cyclohexane-1,5′-tetrazolo[1,5-c]quinazoline] (**a2**)*

Light-yellow solid in 82.89% yield, mp 196–198°C. ^{1}H NMR (400 MHz): δ (ppm) 7.79 (d, *J* = 7.7 Hz, 1H, H-10), 7.30 (t, *J* = 7.8 Hz, 1H, H-8), 7.07 (d, *J* = 7.5 Hz, 2H, H-7, NH), 6.86 (t, *J* = 7.5 Hz, 1H, H-9), 2.02–2.20 (m, 4H, $C(CH_2)_2(CH_2)_2$), 1.87–1.72 (m, 4H, $C(CH_2)_2(CH_2)_2$), 1.67 (tt, *J* = 8.6, 4.3 Hz, 1H, $C(CH_2)_2(CH_2)_2CH_2$), 1.47 (ddt, *J* = 14.2, 9.5, 5.2 Hz, 1H, $C(CH_2)_2(CH_2)_2CH_2$). IR (cm^{-1}): 1616, 1480, 1246, 1107, 1007, 775, 748, 719, 691. LC-MS: *m/z* = 242 $[M+H]^+$. Anal. calcd. for $C_{13}H_{15}N_5$: C, 64.71; H, 6.27; N, 29.02. Found: C, 64.67; H, 6.34; N, 28.96.

*6′H-Spiro[indoline-3,5′-tetrazolo[1,5-c]quinazolin]-2-one (**b1**)*

Light-yellow solid in 86.05% yield, mp 275–277°C. ^{1}H NMR (400 MHz) δ 10.77 (s, 1H, NH(indole)), 8.01 (s, 1H NH(quinaz.)), 7.88 (d, *J* = 7.7 Hz, 1H, H-10), 7.44 (d, *J* = 8.1 Hz, 2H, indole H-4,5), 7.35 (t, *J* = 7.9 Hz, 1H, H-8), 7.12 (t, *J* = 7.6 Hz, 1H, indole H-6), 7.04 (d, *J* = 7.8 Hz, 1H, H-7), 6.98–6.83 (m, 2H, H-9, indole H-7). IR (cm^{-1}): 1716, 1621, 1474, 749. LC-MS: *m/z* = 291 $[M+H]^+$. Anal. calcd. for $C_{15}H_{10}N_6O$: C, 62.06; H, 3.47; N, 28.95. Found: 62.11; H, 3.44; N, 28.98.

N-*(3-Chlorophenyl)-2-(2-oxo-6′H-spiro[indoline-3,5′-tetrazolo[1,5-c]quinazolin]-1-yl)-acetamide (**b2**)*

Beige solid in 87.32% yield, mp 242–244°C. IR (cm^{-1}): 1726, 1678, 1616, 1471, 748, 682. ^{1}H NMR (400 MHz). δ 10.48 (s, 1H, NH), 8.18 (s, 1H, NH(quinaz.)), 7.89 (d, *J* = 7.7 Hz, 1H, H-10), 7.79 (d, *J* = 2.5 Hz, 1H, indole H-4), 7.55 (dd, *J* = 10.2, 7.3 Hz, 2H, indole H-5, Ph-2), 7.44 (d, *J* = 8.3 Hz, 1H, Ph-6), 7.36 (t, *J* = 7.7 Hz, 1H, H-8), 7.30–7.16 (m, 2H, Ph-4,5), 7.03 (m, 2H, H-7, indole H-6), 6.97–6.88 (m, 2H, H-9, indole H-7), 4.57 (q, *J* = 16.9 Hz, 2H, CH_2). LC-MS: *m/z* = 458 $[M+H]^+$. Anal. calcd. for $C_{23}H_{16}ClN_7O_2$: C, 60.33; H, 3.52; N, 21.41. Found: C, 60.35; H, 3.49; N, 21.44.

*2-(2-Oxo-6′H-spiro[indoline-3,5′-tetrazolo[1,5-c]quinazolin]-1-yl)-N-(2-(trifluoromethyl)-phenyl)acetamide (**b3**)*

Light-brown solid in 90.31% yield, mp 119–121°C. ^{1}H NMR (400 MHz) δ 8.77 (t, *J* = 6.2 Hz, 1H, $NHCH_2$), 8.13 (s, 1H, NH (quinaz.)), 7.90 (d, *J* = 7.7 Hz, 1H, H-10), 7.65 (t, *J* = 8.8 Hz, 1H, Ph-3), 7.61–7.50 (m, 3H, indole H-4,5, Ph-4), 7.43 (t, *J* = 7.6 Hz, 1H, Ph-6), 7.36 (t, *J* = 7.9 Hz, 1H, H-8), 7.23 (t, *J* = 7.5 Hz, 1H, indole H-6), 7.15 (d, *J* = 7.9 Hz, 1H, H-7), 7.02–6.90 (m, 3H, H-9, indole H-7, Ph-5), 4.52–4.39 (m, 4H, NCH_2, $NHCH_2$). IR (cm^{-1}): 1665, 1620, 1470, 1314, 1163, 1099, 1037, 748. LC-MS: *m/z* = 506 $[M+H]^+$. Anal. calcd. for $C_{25}H_{18}F_3N_7O_2$: C, 59.41; H, 3.59; N, 19.40. Found: C, 59.46; H, 3.56; N, 19.45.

*5-(p-Tolyl)-5,6-dihydrotetrazolo[1,5-c]quinazoline (**c1**)*

Beige solid in 85.78% yield, mp 201–203°C. ^{1}H NMR (400 MHz): δ (ppm): 7.82 (d, *J* = 7.7 Hz, 1H, H-10), 7.65 (s, 1H, NH), 7.33 (m, 3H, Ph-2,6, H-8), 7.21 (d, *J* = 7.8 Hz, 2H, Ph-3,5), 7.08 (s, 1H, CH), 6.99 (d, *J* = 8.2 Hz, 1H, H-7), 6.87 (t, *J* = 7.5 Hz, 1H, H-9), 2.36 (s, 3H, CH_3). ^{13}C NMR (125 MHz): δ (ppm): δ 149.21 (C1a), 144.02 (C6a), 139.87 (C14), 135.24 (C11), 133.83 (C8), 129.87 (C13,15), 127.47 (C11,16), 125.43 (C10), 119.43 (C9), 115.68 (C7), 106.95 (C10a), 71.18 (C5), 21.25 (CH_3). IR (cm^{-1}): 1621, 1481, 1090, 794, 767, 748. LC-MS: *m/z* = 264 $[M+H]^+$. Anal. calcd. for $C_{15}H_{13}N_5$: C, 68.42; H, 4.98; N, 26.60. Found: C, 68.49; H, 4.93; N, 26.66.

*5-(4-Chlorophenyl)-5,6-dihydrotetrazolo[1,5-c]quinazoline (**c2**)*

Beige solid in 90.96% yield, mp 204–206°C. ^{1}H NMR (400 MHz): δ (ppm): 7.83 (d, *J* = 7.7 Hz, 1H, H-10), 7.71 (s, 1H, NH), 7.43 (q, *J* = 8.3 Hz, 4H, Ph-2,3,5,6), 7.33 (t, *J* = 7.8 Hz, 1H, H-8), 7.19 (d, *J* = 1.8 Hz, 1H, CH), 6.99 (d, *J* = 8.2 Hz, 1H, H-7), 6.88 (t, *J* = 7.6 Hz, 1H, H-9). ^{13}C NMR (125 MHz, DMSO-d6) δ 149.50 (C1a), 144.02 (C6a), 136.15 (C14), 134.09 (C11), 133.85 (C8), 132.52 (C13), 130.84 (C15), 128.99 (C10), 125.43, (C12) 123.10 (C16), 119.29 (C9), 115.40 (C7), 106.46 (C10a), 71.78 (C5). IR (cm^{-1}): 3745, 2378, 1691, 1625, 1548, 1483, 1249, 1085, 1014, 828, 798, 771, 749, 645. LC-MS: *m/z* = 284 $[M+H]^+$. Anal. calcd. for $C_{14}H_{10}ClN_5$: C, 59.27; H, 3.55; N, 24.68. Found: C, 59.22; H, 3.59; N, 24.64.

*5-Methyl-5-phenyl-5,6-dihydrotetrazolo[1,5-c]quinazoline (**c3**)*

Brown solid in 50.86% yield, mp 177–179°C. ^{1}H NMR (400 MHz): δ (ppm) 8.07 (s, 1H, NH), 7.75 (d, *J* = 7.7 Hz, 1H, H-10), 7.35–7.14 (m, 6H, Ph-2,3,4,5,6, H-8), 7.05 (d, *J* = 8.2 Hz, 1H, H-7), 6.84 (t, *J* = 7.5 Hz, 1H, H-9), 2.30 (s, 3H, CH_3). ^{13}C NMR (125 MHz): δ (ppm): 149.10 (C 1a), 143.28 (C6a), 142.99 (C14), 134.03 (C11), 129.21 (C13,C15), 128.99 (C8), 125.50 (C10), 125.06 (C12, C16), 119.90 (C9), 116.03 (C7), 107.72 (C10a), 77.16 (C5), 28.78 (CH_3). IR (cm^{-1}): 1622, 1495, 1220, 751, 695. LC-MS: *m/z* = 264 $[M+H]^+$. Anal. calcd. for $C_{15}H_{13}N_5$: C, 68.42; H, 4.98; N, 26.60. Found: C, 68.49; H, 4.91; N, 26.68.

*5-(2-Chlorophenyl)-5-methyl-5,6-dihydrotetrazolo[1,5-c] quinazoline (**c4**)*

Light-brown solid in 62.30% yield, mp 185–187°C. ^{1}H NMR (400 MHz): δ (ppm): 7.81 (d, *J* = 7.7 Hz, 1H, H-10), 7.71 (s, 1H, NH), 7.41 (d, *J* = 7.7 Hz, 1H, Ph-6), 7.35 (t, 1H, *J* = 7.7 Hz, H-8), 7.29 (q, *J* = 6.9 Hz, 2H, Ph-3,5), 6.97–6.82 (m, 3H, H-7,9, Ph-4), 2.34 (s, 3H, CH_3). ^{13}C NMR (125 MHz): δ (ppm): 149.18 (C1a), 142.75 (C6a), 137.63 (C14), 133.94 (C11), 133.13 (C8), 132.48 (C13,15), 131.57

(C10), 128.83 (C12,C16), 127.72 (C9), 125.40 (C12, C16), 119.16 (C7), 115.54 (C10a), 76.85 (C5), 27.92 (CH_3). IR (cm^{-1}): 1627, 1552, 1503, 1041, 768, 749. LC-MS: m/z = 298 $[M+H]^+$. Anal. calcd. for $C_{15}H_{12}ClN_5$: C, 60.51; H, 4.06; Cl, 11.91; N, 23.52. Found: C, 60.58; H, 4.01; Cl, 11.95; N, 23.47.

*5-(4-Bromophenyl)-5-methyl-5,6-dihydrotetrazolo[1,5-c] quinazoline (**c5**)*

Beige solid in 83.63% yield, mp 221–223°C. ^1H NMR (400 MHz): δ (ppm): 8.09 (s, 1H, NH), 7.75 (d, J = 7.4 Hz, 1H, H-10), 7.41 (d, J = 8.5 Hz, 2H, Ph-2,6), 7.37 (t, J = 7.5 Hz, 1H, H-8), 7.10 (d, J = 8.6 Hz, 2H, Ph-3,5), 7.04 (d, J = 8.2 Hz, 1H, H-7), 6.86 (t, J = 7.5 Hz, 1H, H-9), 2.29 (s, 3H, CH_3). IR (cm^{-1}): 476, 1078, 1006, 810, 749. LC-MS: m/z = 344 $[M+H]^+$. Anal. calcd. for $C_{15}H_{12}BrN_5$: C, 52.65; H, 3.53; N, 20.47. Found: C, 52.61; H, 3.59; N, 20.43.

*4-(5-Methyl-5,6-dihydrotetrazolo[1,5-c]quinazolin-5-yl)phenol (**c6**)*

Beige solid in 40.44% yield, mp 190–194°C. ^1H NMR (400 MHz): δ (ppm): 9.25 (s, 1H, OH), 7.90 (s, 1H, NH), 7.74 (d, J = 7.7 Hz, 1H, H-10), 7.30 (t, J = 7.5 Hz, H-8), 7.02 (d, J = 8.3 Hz, 1H, H-7), 6.98 (d, J = 8.5 Hz, 2H, Ph-2,6), 6.84 (t, J = 7.2 Hz, 1H, H-9), 6.62 (dd, J = 8.4, 6.3 Hz, 2H, Ph-3,5), 2.24 (s, 3H, CH_3). IR (cm^{-1}): 1623, 1496, 1228, 1176, 837, 751. LC-MS: m/z = 280 $[M+H]^+$. Anal. calcd. for $C_{15}H_{13}N_5O$: C, 64.51; H, 4.69; N, 25.07; O, 5.73. Found: C, 64.58; H, 4.63; N, 25.13; O, 5.68.

*4-(5-Methyl-5,6-dihydrotetrazolo[1,5-c]quinazolin-5-yl) benzonitrile (**c7**)*

Light-brown solid in 83.15% yield, mp 229–231°C. ^1H NMR (400 MHz): δ (ppm) 8.21 (s, 1H, NH), 7.76 (d, J = 7.7 Hz, 1H, H-10), 7.67 (d, J = 8.1 Hz, 2H Ph-2,6), 7.38–7.30 (m, 3H, Ph-3,5, H-8), 7.05 (d, J = 8.2 Hz, 1H, H-7), 6.87 (t, J = 7.5 Hz, 1H, H-9), 2.32 (s, 3H, CH_3). IR (cm^{-1}): 1621, 1477, 1214, 1112, 1078, 835, 753, 615. LC-MS: m/z = 289 $[M+H]^+$. Anal. calcd. for $C_{16}H_{12}N_6$: C, 66.66; H, 4.20; N, 29.15. Found: C, 66.69; H, 4.17; N, 29.17.

*5-Methyl-5-(4-nitrophenyl)-5,6-dihydrotetrazolo[1,5-c] quinazoline (**c8**)*

Light-brown solid in 67.79% yield, mp 247–249°C. ^1H NMR (400 MHz): δ (ppm) 8.26 (s, 1H, NH), 8.13 (d, J = 8.5 Hz, 2H, Ph-2,6), 7.76 (d, J = 7.7 Hz, 1H, H, H-10), 7.41 (d, J = 8.5 Hz, 2H, Ph-3,5), 7.35 (t, J = 7.8 Hz, 1H, H-8), 7.06 (d, J = 8.2 Hz, 1H, H-7), 6.88 (t, J = 7.5 Hz, 1H, H-9), 2.35 (s, 3H, CH_3). IR (cm^{-1}): 1621, 1518, 1348, 1111, 853, 802, 776, 755, 698. LC-MS: m/z = 309 $[M+H]^+$. Anal. calcd. for $C_{15}H_{12}N_6O_2$: C, 58.44; H, 3.92; N, 27.26; O, 10.38. Found: C, 58.49; H, 3.86; N, 27.32; O, 10.34.

*3-(5-Methyl-5,6-dihydrotetrazolo[1,5-c]quinazolin-5-yl)benzoic acid (**c9**)*

Beige solid in 53.54% yield, mp 278–280°C. ^1H NMR (400 MHz): δ (ppm): 12.78 (s, 1H, COOH), 8.18 (s, 1H, NH), 7.87 (s, 1H, Ph-2), 7.84 (d, J = 7.8 Hz, 1H, Ph-4), 7.75 (d, J = 7.7 Hz, 1H, H-10), 7.40–7.32 (m, 2H, Ph-5,6), 7.29 (t, J = 7.8 Hz, 1H, H-8), 7.06 (d, J = 8.2 Hz, 1H, H-7), 6.85 (t, J = 7.5 Hz, 1H, H-9), 2.32 (s, 3H, CH_3). IR (cm^{-1}): 3852, 3743, 1682, 1625, 1506, 1212, 751, 721, 669. LC-MS: m/z = 308 $[M+H]^+$. Anal. calcd. for $C_{16}H_{13}N_5O_2$: C, 62.53; H, 4.26; N, 22.79; O, 10.41. Found: C, 62.59; H, 4.20; N, 22.84; O, 10.35.

*4-(5-Methyl-5,6-dihydrotetrazolo[1,5-c]quinazolin-5-yl)benzoic acid (**c10**)*

Beige solid in 62.98% yield, mp 274–278°C. ^1H NMR (400 MHz): δ (ppm): 12.65 (s, 1H, COOH), 8.15 (s, 1H, NH), 7.86 (d, J = 8.2 Hz, 2H, Ph-3,5), 7.75 (d, J = 7.7 Hz, 1H, H-10), 7.32 (t, J = 7.7 Hz, 1H, H-8), 7.24 (d, J = 8.1 Hz, 2H, Ph-2,6), 7.05 (d, J = 8.2 Hz, 1H, H-7), 6.85 (t, J = 7.5 Hz, 1H, H-9), 2.32 (s, 3H, CH_3). ^{13}C NMR (125 MHz): δ (ppm): 167.02 (COOH), 149.11 (C1a), 147.41 (C6a), 142.99 (C14), 134.10 (C11), 131.53 (C8), 130.25 (C13,C15), 125. 94 (C12,C16), 125.43 (C10), 120.10 (C9), 116.10 (C7), 107.69 (C10a), 76.97 (C5), 28.45 (CH_3). IR (cm^{-1}): 3856, 3745, 1693, 1625, 1501, 1213, 1111, 856, 745, 703. LC-MS: m/z = 308 $[M+H]^+$. Anal. calcd. for $C_{16}H_{13}N_5O_2$: C, 62.53; H, 4.26; N, 22.79; O, 10.41. Found: C, 62.59; H, 4.22; N, 22.85; O, 10.36.

*5-Methyl-5-(pyridin-2-yl)-5,6-dihydrotetrazolo[1,5-c] quinazoline (**d1**)*

Light-yellow solid in 92.16% yield, mp 212–214°C. ^1H NMR (400 MHz): δ (ppm): 8.44 (d, J = 5.3 Hz, 1H, Pyr-6), 8.01 (s, 1H, NH), 7.76 (d, 1H, H-10), 7.69 (t, J = 7.8 Hz, 1H, Pyr-4), 7.31–7.19 (m, 2H, H-8, Pyr-5), 7.12 (d, J = 8.0 Hz, 1H, H-7), 6.97 (d, J = 8.2 Hz, 1H, Pyr-3), 6.82 (t, J = 7.5 Hz, 1H, H-9), 2.33 (s, 3H, CH_3). IR (cm^{-1}): 1622, 1504, 1474, 1103, 783, 747, 719. ^{13}C NMR (125 MHz): δ (ppm): 160.03 (C1a), 149.39 (C11), 149.40 (C15), 142.99 (C6a), 138.08 (C13), 133.71 (C8), 125.37 (C10), 124.15 (C9), 119.77 (C14), 119.46 (C12), 115.83 (C7), 107.80 (C10a), 77.35 (C5), 26.67 (CH_3). LC-MS: m/z = 265 $[M+H]^+$. Anal. calcd. for $C_{14}H_{12}N_6$: C, 63.62; H, 4.58; N, 31.80. Found: C, 63.68; H, 4.52; N, 31.86.

*5-Methyl-5-(pyridin-3-yl)-5,6-dihydrotetrazolo[1,5-c] quinazoline (**d2**)*

Light-brown solid in 42.72% yield, mp 210–212°C. ^1H NMR (400 MHz): δ (ppm): 8.45 (brs, 1H, Pyr-2), 8.43 (d, J = 5.3 Hz, 1H, Pyr-6), 8.15 (s, 1H, NH), 7.78 (d, J = 7.7 Hz, 1H, H-10), 7.48 (dt, J = 8.3, 2.0 Hz, 1H, Pyr-4), 7.35 (t, J = 7.8 Hz, 1H, H-8), 7.26 (dd, J = 8.1, 4.7 Hz, 1H, Pyr-5), 7.07 (d, J = 8.2 Hz, 1H, H-7), 6.88 (t, J = 7.5 Hz, 1H, H-9), 2.34 (s, 3H, CH_3). IR (cm^{-1}): 1621, 1476, 1420, 1378, 1232, 1079, 809, 775, 751, 713. LC-MS: m/z = 265 $[M+H]^+$. Anal. calcd. for $C_{14}H_{12}N_6$: C, 63.62; H, 4.58; N, 31.80. Found: C, 63.65; H, 4.56; N, 31.83.

*5-Methyl-5-(pyridin-4-yl)-5,6-dihydrotetrazolo[1,5-c] quinazoline (**d3**)*

Light-brown solid in 19.53% yield, mp 178–180°C. ^1H NMR (400 MHz): δ (ppm): 8.58 (d, J = 5.4 Hz, 2H, Pyr-2,6), 8.33 (s, 1H, NH), 7.77 (d, J = 7.7 Hz, 1H, H-10), 7.35 (t, J = 7.8 Hz, 1H, H-8), 7.29 (d, J = 5.5 Hz, 2H, Pyr-3,5), 7.10 (d, J = 8.2 Hz, 1H, H-7), 6.88 (t, J = 7.5 Hz, 1H, H-9), 2.34 (s, 3H, CH_3). IR (cm^{-1}): 1659, 1622,

1482, 1383, 1212, 1087, 815, 754. LC-MS: m/z = 265 $[M+H]^+$. Anal. calcd. for $C_{14}H_{12}N_6$: C, 63.62; H, 4.58; N, 31.80. Found: C, 63.64; H, 4.56; N, 31.86.

4.3 | Molecular docking studies

Macromolecules from Protein Data Bank (PDB) were used as a biological targets, namely, of 50S ribosomal protein L19 from *S. aureus* (PDB ID: 6WQN),[28] sterol 14-alpha demethylase from *C. albicans* (PDB ID: 5TZ1),[29] and ras-related protein Rab-9A from (PDB ID: 1WMS) from *Homo sapiens*.[32] Tedizalid[24] and oteseconazole[25] were chosen as the references. The 20 mol files of 5,6-dihydrotetrazolo[1,5-c] quinazoline derivatives and reference compounds were drawn by MarvinSketch 20.20.0 and saved in mol format; optimized by HyperChem 8.0.8; mol files were converted to pdb by Open Babel GUI 2.3.2; pdb files were converted to pdbqt by AutoDocTools 1.5.6. Vina 1.1.2 was used to carry out docking studies.[54] The following grid box was used for 6WQN: center_x = 205.105, center_y = 180.986, center_z = 163.855, size_x = 10, size_y = 10, size_z = 16; for 1WMS: center_x = -0.285, center_y = 21.447, center_z = 7.411, size_x = 14, size_y = 14, size_z = 14; for 5TZ1: center_x = 70.6098, center_y = 66.2844, center_z = 4.1774, size_x = 14, size_y = 16, size_z = 14. Discovery Studio v17.2.0.16349 was used for visualization.

To validate the docking method by the value of root-mean-squared deviation (RMSD), which characterizes the degree of reliable docking probability, the reference ligands were extracted and then reused for the redocking process.[55] If the found pose has a RMSD less than 2Å relative to the X-ray conformation, then it is generally considered a docking success.[56] RSMD values between the experimental and the reference conformation ligands were calculated to be 0.983 Å for PDB ID: 1WMS, and 1.731 Å for PDB ID: 5TZ1, and 1.974 Å for PDB ID: 6WQN via DockRMSD available online.[57] Therefore, the studies are considered as reliable.

4.4 | Antimicrobial studies

The method of serial dilutions (2–256 mg/L) on meat-peptone broth,[49,58] was carried out in the bacteriological laboratory of Zaporizhzhia Regional Clinical Hospital (Zaporizhzhia, Ukraine) against *S. aureus* ATCC 25923 F-49, *E. coli* ATCC 25922, *P. aeruginosa* ATCC 27863, *Klebsiella (Enterobacter) aerogenes* and *C. albicans* ATCC 885-653. All growth experiments were carried out in duplicate

4.5 | Targets prediction

Super-PRED, a prediction webserver for targets prediction[51] and ATC codes[33] of compounds, was used. The ATC code prediction is based on machine learning, using a linear logistic regression model. It is trained on Morgan fingerprints from 1552 different drugs in 233 different level 4 ATC classes. Query compounds are evaluated and scored by the machine learning model, ranking each ATC class and returning the highest scoring classes. The webserver's target prediction is based on a machine learning model, using logistic regression and Morgan fingerprints of length 2048.

ACKNOWLEDGMENTS

The work was performed with the technical support of Enamine Ltd (Kyiv, Ukraine). Authors gratefully acknowledge the Armed Forces of Ukraine and Territorial Defense Forces of the Armed Forces of Ukraine for preparing this paper in the safe conditions of Zaporizhzhia, Ukraine. The authors gratefully acknowledge the National University Corporation Kyushu University, Fukuoka, Japan, for the opportunity to take part in the relief program for Ukrainian students and researchers.

CONFLICTS OF INTEREST STATEMENT

The authors declare no conflicts of interest.

ORCID

Lyudmyla Antypenko http://orcid.org/0000-0003-0057-1551
Oleksii Antypenko http://orcid.org/0000-0002-8048-445X
Oksana Rebets http://orcid.org/0000-0002-7328-3481
Sergiy Kovalenko http://orcid.org/0000-0001-8017-9108
Mieko Arisawa http://orcid.org/0000-0002-9561-2653

REFERENCES

[1] O. Sköld, *Antibiotics and Antibiotic Resistance*, John Wiley & Sons, Inc, **2011**.
[2] C. Gao, L. Chang, Z. Xu, X. F. Yan, C. Ding, F. Zhao, X. Wu, L. S. Feng, *Eur. J. Med. Chem.* **2019**, *163*, 404. https://doi.org/10.1016/j.ejmech.2018.12.001
[3] N. Kaushik, N. Kumar, A. Kumar, U. K. Singh, *Immunol. Endocr. Metab. Agents Med. Chem.* **2018**, *18*, 3. https://doi.org/10.2174/1871522218666180525100850
[4] A. M. Young, K. L. Audus, J. Proudfoot, M. Yazdanian, *J. Pharm. Sci.* **2006**, *95*, 717. https://doi.org/10.1002/jps.20526
[5] L. V. Myznikov, A. Hrabalek, G. I. Koldobskii, *Chem. Heterocycl. Compds.* **2007**, *43*, 1. https://doi.org/10.1007/S10593-007-0001-5
[6] P. Kushwaha, S. Fatima, A. Upadhyay, S. Gupta, S. Bhagwati, T. Baghel, M. I. Siddiqi, A. Nazir, K. V. Sashidhara, *Bioorg. Med. Chem. Lett.* **2019**, *29*(1), 66. https://doi.org/10.1016/j.bmcl.2018.11.005
[7] Y. Li, K. K. Pasunooti, R. J. Li, W. Liu, S. A. Head, W. Q. Shi, J. O. Liu, *J. Med. Chem.* **2018**, *61*(24), 11158. https://doi.org/10.1021/acs.jmedchem.8b01252
[8] J. Zhang, S. Wang, Y. Ba, Z. Xu, *Eur. J. Med. Chem.* **2019**, *178*, 341. https://doi.org/10.1016/j.ejmech.2019.05.071
[9] G. Belz, *Clin. Pharm. Ther.* **1999**, *66*, 367. https://doi.org/10.1053/cp.1999.v66.a101162
[10] P. Zhan, Z. Li, X. Liu, E. De Clercq, *Mini-Rev. Med. Chem.* **2009**, *9*(8), 1014. https://doi.org/10.2174/138955709788681618
[11] F. Gao, J. Xiao, G. Huang, *Eur. J. Med. Chem.* **2019**, *184*, 111744. https://doi.org/10.1016/j.ejmech.2019.111744
[12] J. Roh, G. Karabanovich, H. Vlčková, A. Carazo, J. Němeček, P. Sychra, L. Valášková, O. Pavliš, J. Stolaříková, V. Klimešová, K. Vávrová, P. Pávek, A. Hrabálek, *Bioorg. Med. Chem.* **2017**, *25*(20), 5468. https://doi.org/10.1016/j.bmc.2017.08.010
[13] L. M. Antypenko, *Sci. Pharm.* **2013**, *81*, 15. https://doi.org/10.3797/scipharm.1208-13

[14] O. M. Antypenko, I. M. Vasileva, S. I. Kovalenko, *Curr. Issues Pharm. Med. Sci. Practice* **2016**, (21), 62. https://doi.org/10.14739/2409-2932.2016.2.70903
[15] O. M. Antypenko, L. M. Antypenko, S. I. Kovalenko, A. M. Katsev, O. M. Achkasova, *Arabian J. Chem.* **2016**, *9*(6), 792. https://doi.org/10.1016/j.arabjc.2014.09.009
[16] A. Kamal, K. S. Babu, Y. Poornachandra, B. Nagaraju, S. M. Ali Hussaini, S. P. Shaik, C. Ganesh Kumar, A. Alarifi, *Arabian J. Chem.* **2019**, *12*(8), 3546. https://doi.org/10.1016/j.arabjc.2015.10.013
[17] R. Zanni, M. Galvez-Llompart, R. Garcia-Domenech, J. Galvez, *Expert Opin. Drug Discov.* **2020**, *15*, 1133. https://doi.org/10.1080/17460441.2020.1770223
[18] R. S. Bohacek, C. McMartin, W. C. Guida, *Med. Res. Rev.* **1996**, *16*(1), 3. https://doi.org/10.1002/(SICI)1098-1128(199601)16:1%3C3::AID-MED1%3E3.0.CO;2-6
[19] G. L. Wilson, M. A. Lill, *Future Med. Chem.* **2011**, *3*(6), 735. https://doi.org/10.4155/fmc.11.18
[20] S. G. Buchanan, *Curr. Opin. Drug Discov. Dev.* **2002**, *5*(3), 367. https://europepmc.org/article/med/12058612
[21] S. Singh, B. K. Malik, D. K. Sharma, *Bioinformation* **2006**, *1*(8), 314. https://doi.org/10.6026/97320630001314
[22] A. A. Carena, M. E. Stryjewski, *Expert Rev. Clin. Pharmacol.* **2020**, *13*(6), 577. https://doi.org/10.1080/17512433.2020.1774362
[23] Tedizolid Phosphate. *Drugbank Online*. **2023**. https://go.drugbank.com/drugs/DB09042
[24] M. Roch, M. C. Varela, A. Taglialegna, A. E. Rosato, *J. Antimicrob. Chemother.* **2020**, *75*(1), 126. https://doi.org/10.1093/jac/dkz418
[25] J. D. Sobel, P. Nyirjesy, *Future Microbiol.* **2021**, *16*, 1453. https://doi.org/10.2217/fmb-2021-0173
[26] W. A. Schell, A. M. Jones, E. P. Garvey, W. J. Hoekstra, R. J. Schotzinger, B. D. Alexander, *Antimicrob. Agents Chemother.* **2017**, *61*(3), e01817. https://doi.org/10.1128/AAC.01817-16
[27] E. P. Garvey, W. J. Hoekstra, R. J. Schotzinger, J. D. Sobel, E. A. Lilly, P. L. Jr. Fidel, *Antimicrob. Agents Chemother.* **2015**, *59*(9), 5567. https://doi.org/10.1128/AAC.00185-15
[28] 6WQN. *Structure of the 50S Subunit of the Ribosome from Methicillin Resistant Staphylococcus aureus in Complex with the Antibiotic, Contezolid*. https://www.rcsb.org/structure/6WQN
[29] 5TZ1. *Crystal Structure of Sterol 14-Alpha Demethylase (CYP51) from Candida albicans in Complex with the Tetrazole-Based Antifungal Drug Candidate VT1161 (VT1)*. https://www.rcsb.org/structure/5TZ1
[30] W. J. Hoekstra, E. P. Garvey, W. R. Moore, S. W. Rafferty, C. M. Yates, R. J. Schotzinger, *Bioorg. Med. Chem. Lett.* **2014**, *24*(15), 3455. https://doi.org/10.1016/j.bmcl.2014.05.068
[31] M. M. Teixeira, D. T. Carvalho, E. Sousa, E. Pinto, *Pharmaceuticals* **2022**, *15*, 1427. https://doi.org/10.3390/ph15111427
[32] 1WMS. *High Resolution Crystal Structure of Human Rab9 GTPase: A Novel Antiviral Drug Target*. https://www.rcsb.org/structure/1WMS
[33] Super-PRED. *Drug Classification*. **2023**. https://prediction.charite.de/subpages/classification.php
[34] UniProt. **2023**. https://www.uniprot.org/uniprotkb/P51151/entry
[35] B. Kowalska-Krochmal, R. Dudek-Wicher, *Pathogens* **2021**, *10*(2), 165. https://doi.org/10.3390/pathogens10020165
[36] P. Ertl, E. Altmann, J. M. McKenna, *J. Med. Chem.* **2020**, *63*(15), 8408. https://doi.org/10.1021/acs.jmedchem.0c00754
[37] E. R. Wagner, *US3835138*, **1974**.
[38] Y. Liu, X. Qi, W. Zhang, P. Yin, Z. Cai, Q. Zhang, *Org. Lett.* **2021**, *23*(3), 734. https://doi.org/10.1021/acs.orglett.0c03952
[39] K. M. Amin, M. M. Anwar, Y. M. Syam, M. A. Khedr, M. M. Kamel, E. M. Kassem, *Acta Pol. Pharm.* **2013**, *70*(4), 687.
[40] H.-K. Fun, C. S. Yeap, J. Gowda, A. M. A. Khader, B. Kalluraya, *Acta Crystallogr. Sect. E. Struct. Rep. Online*. **2010**, *E66*, o3219. https://doi.org/10.1107/S160053681004688X
[41] P. G. V. V. Lakshmi, N. T. Patil, *Asian J. Chem.* **2014**, *26*(10), 2971. https://doi.org/10.14233/ajchem.2014.16157
[42] Drugbank Online. **2023**. https://go.drugbank.com/structures/search/small_molecule_drugs/structure#results
[43] Protox II. **2022**. https://tox-new.charite.de/protox_II/index.php?site=compound_input
[44] P. Banerjee, A. O. Eckert, A. K. Schrey, R. Preissner, *Nucleic Acids Res.* **2018**, *46*(1), W257. https://doi.org/10.1093/nar/gky318
[45] Celecoxib. *Common Chemistry*. **2022**. https://commonchemistry.cas.org/detail?cas_rn=169590-42-5
[46] Fluoxetine. *Common Chemistry*. **2022**. https://commonchemistry.cas.org/detail?cas_rn=54910-89-3
[47] N. Cosdon. *FDA Approves Oteseconazole, First and Only Treatment for Chronic Yeast Infection*. **2022**. https://www.contagionlive.com/view/fda-approves-oteseconazole-first-and-only-treatment-for-chronic-yeast-infection.
[48] C. G. Neochoritis, T. Zhao, A. Dömling, *Chem. Rev.* **2019**, *119*(3), 1970. https://doi.org/10.1021/acs.chemrev.8b00564
[49] Л. Антипенко, Р. Оксана, І. Карнаух, О. Антипенко, С. Коваленко, *Grail Sci.* **2022**, *17*, 468. https://doi.org/10.36074/grail-of-science.22.07.2022.082
[50] Olmesartan. *DRUGBANK Online*. **2023**. https://go.drugbank.com/drugs/DB00275
[51] Super PRED. *Targets Prediction*. **2022**. https://prediction.charite.de/subpages/target_prediction.php
[52] O. Antypenko, L. Antypenko, D. Kalnysh, S. Kovalenko, *Grail Sci.* **2022**, *12-13*, 684. https://doi.org/10.36074/grail-of-science.29.04.2022.124
[53] J. B. Baell, G. A. Holloway, *J. Med. Chem.* **2010**, *53*, 2719. https://doi.org/10.1021/jm901137j
[54] O. Trott, A. J. Olson, *J. Comput. Chem.* **2009**, *31*, 455. https://doi.org/10.1002/jcc.21334
[55] J. C. Baber, D. C. Thompson, J. B. Cross, C. Humblet, *J. Chem. Inf. Model.* **2009**, *49*(8), 1889. https://doi.org/10.1021/ci9001074
[56] G. L. Warren, C. W. Andrews, A.-M. Capelli, B. Clarke, J. LaLonde, M. H. Lambert, M. Lindvall, N. Nevins, S. F. Semus, S. Senger, G. Tedesco, I. D. Wall, J. M. Woolven, C. E. Peishoff, M. S. Head, *J. Med. Chem.* **2006**, *49*(20), 5912. https://doi.org/10.1021/jm050362n
[57] DockRMSD. *Docking Pose Distance Calculation*. **2022**. https://seq.2fun.dcmb.med.umich.edu//DockRMSD
[58] EUCAST. *MIC Determination of Non-fastidious and Fastidious Organisms*. **2022**. https://eucast.org/ast_of_bacteria/mic_determination/

SUPPORTING INFORMATION

Additional supporting information can be found online in the Supporting Information section at the end of this article.

How to cite this article: L. Antypenko, O. Antypenko, I. Karnaukh, O. Rebets, S. Kovalenko, M. Arisawa, *Arch. Pharm.* **2023**, e2300029. https://doi.org/10.1002/ardp.202300029